INFLUENCE OF SURFACE ROUGHNESS ON THE DYNAMIC STALL OF A ROTARY WING SECTION IN SUBSONIC FLOW

Dr. Farag Mahel Mohammed*

ABSTRACT

Wear involves the losses of some material from the surface and leads to the surface roughness. In the present work, the influence of surface roughness on the dynamic stall of a rotary wing section in subsonic flow has been investigated with different degree of surface roughness. The airfoil surface roughness was estimated using arithmetic mean roughness value (ISO-4287/1). For this purpose an indicial response method for unsteady, two dimensional flow is used to calculating the unsteady lift and pitching moment of NACA 0012 airfoil undergoing a pitching oscillation in the deep dynamic stall regime. Using the ANSYS-5.8 software as a source for the preliminary static data that required by the indicial method. The investigation is done through a number of test cases with different mean angles of attack, amplitude and reduced frequencies for airfoil oscillating around its quarter chord axis. The results include the time dependent behaviour and hysteresis loops of the lift and pitching moment for the airfoil with different degree of surface roughness. For rough airfoil an aerodynamic characteristic showed a reduction in the lift coefficient, separation point moved forward to the leading edge, the boundary layer reattachment take place at smaller angle of attack, the stall angle decrease and the pitching moment coefficient decrease as compared with smoother airfoil. So the periodic test must be done and re-coating the rotary wing if the surface roughness increased.

KEYWORDS: dynamic stall, surface roughness, boundary layer

***University of Technology/Education Technology Dept.

SYMBOLS

c Airfoil chord (m).
C_L Lift coefficient.
$C_{L\alpha}$ Static lift-curve slope.
C_m Pitching moment coefficient.
C_{mI} Impulsive pitching moment due to a step change of incidence.
C_{mq} Impulsive pitching moment due to a step change of pitch rate.
C_N Normal force coefficient.
C_{NI} Impulsive normal force coefficient due to a step change of incidence.
C_{Nq} Impulsive normal force coefficient due to a step change of pitch rate.
C_{Nf}^{-} Instantaneous value of the ersatz lift.
Cp Pressure coefficient.
Cpv Center of pressure which is varying with the position of vortex (m).
Cv Normal force coefficient due to vortex lift.
f frequency (Hertz).
L_m Evaluation length (m).
K Reduced frequency (rad).
M Mach number.
R Arithmetic mean roughness value (μm)
Re Reynolds number.
Sep Static separation point.
Sep^{-} Dynamic separation point.
t Time (sec).
V_∞ Free stream velocity(m/sec).
X Chordwise coordinate (m).
α Angle of attack (deg).
α_E Equivalent angle of attack(deg)
α_f^{-} Effective angle of attack (deg)
δ_o Amplitude (deg)
Δq Step change in pitch rate (rad)
Δt Time step (sec)
Φ Wanger function
ω Oscillation frequency (rad/sec).
τ_v Vortex time (sec)

SUBSCRIPTS

f′ Effective
n Time step counter
Sep Condition of separation point

1. INTRODUCTION

Most airfoil surfaces are subjected to wear either in machinery or due to the dusty weather. In many case the surfaces will have some degree of roughness that is concomitant with its finishing process. The performance of the rotary wing section is usually significantly affected by surface roughness. The rotary wing dynamic stall phenomena may be occurring if the angle of attack oscillates around the static stall angle [1]. These oscillations lead to relatively high dynamic pressures corresponding to low angles of attack on the advancing side of the rotor disc, and relatively low dynamic pressures at high angles of attack on the retreating side, figure (1) [2]. The phenomenon of dynamic stall limits the flight envelope of a helicopter and reduces the operation regime of wind energy converter [3].

Yousif A. H., et al. [4] had been investigated the influence of surface roughness on the cascade blade performance characteristics, the results showed that the degree and distribution of roughness eliminate the operating condition of the cascade blades, which reduce the value of the stall and nominal deflection angles. Many investigators using both experimental and theoretical techniques have studied the dynamic stall of

airfoils McCroskey and his Co-workers, [5,6,7] studied experimentally the dynamic stall and unsteady boundary-layer separation in incompressible flow at moderately large Reynolds numbers. By varying the leading edge geometry of a NACA 0012 airfoil, three different types of stall were produced, and the vortex shedding phenomenon was found to be the predominant feature of each. Vladislav Klein et al, [8] present a wind tunnel experiment on the 10-percent-scale model of the F-16XL aircraft included longitudinal static tests, oscillatory and ramp tests in pitch. Shida, et al. [9] studied the dynamic stall of NACA-0012 airfoil oscillating in pitch and having a maximum angle of attack greater than the static stall angle experiences peculiar hysteresis in drag, lift and moment coefficients. Abu-Tabikh, M. I., [10] has been studied the phenomena of dynamic stall and gives a description of a method for modeling of unsteady flow separation over two-dimensional airfoils. The vortex panel method was combined with the discrete vortex method in which the unsteady motion were considered, namely, pitching oscillation, heaving oscillation and sudden change in incidence. Rae′d Abbas [11] study the effect of Nose-Drooping flap on the dynamic stall of a rotary wing section, as one of a proposed dynamic stall control technique, on the unsteady lift and pitching moment for the same airfoil. The results show that the aerodynamic characteristic improved with the Nose-Drooping flap deflection.

In the present work the indicial response method will be used for the analysis. The model must be capable of simulating the unsteady motion of the airfoil and simulating the dynamic movement of the separation point. Although the present indicial method follows the original indicial method by Beddos [12], this method together with its later developments [13,14] is predominantly empirical method. In the present model, the predominancy of empirical data is eliminated by using ANSYS-5.8 software as a source for the preliminary static data required by the indicial method.

The developed method is then used to study the effect of surface roughness, on the unsteady aerodynamic characteristic of the NACA 0012 airfoil under dynamic stall conditions.

2. MATHEMATICAL BACKGROUND

By definition, an indicial function is the response to a disturbance, which is applied instantaneously at time zero and held constant thereafter [12]; that is a disturbance given by a step function. For example, this may be step change in incidence.

If the components of the indicial response are known, then the total response to some arbitrary motion may be derived as follows [15,16]; consider some arbitrary variation of angle of attack as a function of time, and suppose that the lift coefficient response to change in angle of attack is given as shown in figure (2), in which two separate approaches to the indicial lift response are used. One for the initial loading which is impulsive in nature and decays rapidly with time, and another for the circulatory loading which builds up quickly in the first few chord lengths of airfoil travel and tends asymptotically to the appropriate steady state value. The increment in circulatory normal lift response due to a step change in incidence ($\Delta\alpha$), may be written as [16]:

$$C_{NC(t)} = C_{L\alpha}.\Phi(t).\Delta\alpha = C_{L\alpha}.\alpha_E(t) \qquad (1)$$

Wagner [16,17] has obtained the indicial lift response of an airfoil operating in incompressible flow for a step change in angle of attack. The Wagner function may be approximated by the following exponential function:

$$\Phi(t) = 1 - A_1 \exp\left(-A_2 \frac{2V_\infty t}{c}\right) - A_3 \exp\left(-A_4 \frac{2V_\infty t}{c}\right) \quad (2)$$

Where: A_1, A_2, A_3 and A_4 are the coefficients of indicial lift function, Leishman [18]

From equations (1 and 2), the equivalent angle of attack $\alpha_E(t)$ may be written as the instantaneous value of incidence minus two exponentially decaying terms i.e.

$$\alpha_E(t) = \left[1 - A_1 \exp\left(-t\left[A_2\left(1-M^2\right)2\frac{V}{c}\right]\right) - A_3 \exp\left(-t\left[A_4\left(1-M^2\right)2\frac{V}{c}\right]\right)\right].\Delta\alpha \quad (3)$$

The response to a continuously varying incidence may be constructs from an accumulating series of inputs. At time (t_n) the circulatory lift may be obtained with the aid of Duhamnel's superposition principle [16] as follows:

$$C_{NCn} = C_{L\alpha}(\alpha_n - X_n - Y_n) \quad (4)$$

The impulsive loadings comprise the initial loading on the airfoil in response to an instantaneous change of incidence or pitch rate. It is composed of two perturbation modes that:

One is due to a step change of angle of incidence ($\Delta\alpha$) and another due to a step change of pitch rate (Δq). For a step change in incidence ($\Delta\alpha_n$) the impulsive normal lift force is:

$$C_{NIn} = \left(\frac{4K_I T_I}{M}\right)\left(D\alpha_n - DI'_n\right) \quad (5)$$

Similar equations are used for the impulsive normal lift force due to a step change in pitch rate. For the impulsive pitching moment:

$$C_{MIn} = -\frac{C_{NIn}}{4} \quad (6)$$

$$C_{Mqn} = \left(-\frac{C_{Nqn}}{4}\right) - \left(\frac{K_I^2 T_I}{3M}\right)\left(Dq_n - Dq''_n\right) \quad (7)$$

Equations (1 to 7) form the basis of the attached flow portion of the indicial method. Where (X_n, Y_n, T_I, K_I, $D\alpha n$, DI'_n and Dq''_n) are estimated as in reference [13].

3. UNSTEADY SEPARATED FLOW

For a given airfoil at particular Reynolds number, the original indicial method requires the following empirical input data [10,11].

1. The static lift-curve slope ($C_{L\alpha}$).
2. The ratio of the actual lift coefficient to that in attached potential flow, as a function of separation point.
3. The static variation of separation point with the angle of attack.
4. Angle of attack corresponding to the break in the static pitching moment.

3.1 UTILIZATION OF ANSYS-5.8 SOFTWARE

In the present method, the above data required are estimated by means of ANSYS-5.8 program and are then used in the indicial method. Thus, the predominancy of empirical data is eliminated from the present indicial method. The required static data for a given airfoil at a particular Reynolds number are calculated by program ANSYS-5.8 in which the Navier-Stokes equations are solved by finite element method to predict the static lift coefficient, static pitching moment coefficient and drag coefficient as a function of angle of attack. Also the position of static separation point for different angles of attack and surface roughness is calculated.

The total normal force at time (t_n) is,

$$C_{Nn} = C_{NCn} + C_{NIn} + C_{Nqn} \tag{8}$$

At any instant of time, instantaneous value of the ersatz lift ($C_{Nf'_n}$) may be viewed as a value of C_{Nn}, equation (8) minus two exponentially decaying terms. The accumulated response to a series of inputs may be obtained via Duhamnel's superposition principle.

$$C_{Nf'n} = C_{Nn} - DI_n - Df'_n \tag{9}$$

Where DI_n and Df'_n are estimated as in reference [13].

An effective incidence, $\alpha_{f'n}$, is calculated by [16]:

$$\alpha_{f'n} = \frac{C_{Nf'n}}{C_{L\alpha}} \tag{10}$$

The effective incidence is less than the actual incidence during the upstroke of airfoil motion. While during the down stroke is greater than the actual incidence. The dynamic separation point is then obtained from the curve for the static case figure (3) with the aid of cubic spline interpolation procedure.

3.2 UNSTEADY SEPARATION VORTEX EFFECTS

The dynamic stall vortex associated pressure disturbance will induce large changes in the airfoil lift. The vortex lift may be modeled assuming the increment in vortex lift is based on the difference between the instantaneous linear value of the circulatory lift and the corresponding lift as given by an empirical equation representing the non-linear part of the lift curve figure (4).

$$C_{Vn} = C_{NCn}(1 - K_{Nn}) \tag{11}$$

At the same time, the total vortex lift is allowed to decay exponentially with time, but may also be updated by a new increment in lift i.e.:

$$C_{NVn} = C_{NVn-1}\left(\exp\left(-\frac{2V_\infty \Delta t}{cT_V}\right)\right) + (C_{Vn} - C_{Vn-1})\left(\exp\left(-\frac{2V_\infty \Delta t}{cT_V}\right)\right)^{\frac{1}{2}} \tag{12}$$

During the convection of the vortex across the surface of the airfoil, vortex lift is accumulated via the above equations, but is terminated when the vortex reaches the airfoil trailing edge i.e. after a suitable time delay. The center of pressure will vary with the position of vortex [12]. This may be represented by the following equation:

$$Cp_V = 0.25\left[1+\sin\pi\left(\frac{\tau_v}{T_{V1}}-0.5\right)\right] \quad (13)$$

where τ_v is denoted as vortex time, i.e. τ_v=0 at the onset of separation, and τ_v=$TV_1$when the vortex reaches the trailing edge.

The increment in pitching moment due to the vortex lift is given by:

$$C_{MVn} = Cp_V.C_{NVn} \quad (14)$$

During the vortex shedding process, the pressure changes occurring are sufficient to accelerate the forward progression of the separation point. This may be accomplished by halving the time constant associated with the boundary layer response. Thus, the forward movement of the separation point is accelerated if $Sep' < 0.7$ or during the vortex shedding, that is when the vortex time is less than the vortex time limit. Once the vortex passes the trailing edge the lift associated with it decays more rapidly, and this may be modeled by halving the vortex lift time constant T_V for the period $TV_1 < \tau_V < 2TV_1$.

As the incidence decreases, the reattachment process proceeds and loop is repeated. The lift in steady flow may be approximated in terms of the separation point (Sep/c=f) i.e [12].:

$$C_N \approx C_L = 0.25C_{L\alpha}\left(1+\sqrt{f}\right)^2\alpha \quad (15)$$

Thus, if the separation point can be determined, the lift can be estimated [19]. From static test data, the center of pressure at any angle of incidence may be determined from the ratio (C_m/C_N) (allowing for the zero lift moment). The variation can then be plotted versus the corresponding value of the applied separation point and fitted to the form [12]:

$$C_m/C_N = K_o + K_1(1-f) + K_2\sin(\pi f^2) \quad (16)$$

4. SURFACE GEOMETRY

Most airfoil surfaces are subjected to wear either in machinery or due to the dusty weather. In any case the surface will have some degree of roughness that is concomitant with its finishing process. Failure from wear usually involves the loss of some material from the surfaces of solid parts in the system. Wear is a serious cost to the national economy. It only requires the loss of a very small volume of material to render the entire system nonfunctional.

Even an apparently smooth surface will have microscopic irregularities. These can be measured by any of several methods. A number of statistical measures may calculate and ISO defines at least 19. The most commonly used is Arithmetic mean roughness value (ISO-4287/1). The arithmetic average value of filtered roughness profile shown in figure (5) is determined from deviations about the center line within the evaluation length [20].

$$R = \frac{1}{L_m}\int_0^{L_m}|y|dx \quad (17)$$

5. COMPUTATIONAL ALGORITHM

The method of analysis in its form as a computer algorithm has to be simple to both use and understand. The computer programs that satisfy the present method of analysis is written in Fortran 90 language and is given the name SRDTALL. The outline of the computational procedure is:

1. Integrate equation (17) Using Simpson rule numerical integral to compute a hypothetical airfoil surface roughness.
2. Utilization of ANSYS-5.8 software to construct the preliminary static data for the given airfoil at the particular Reynolds and Mach number.
3. Computation of Circulatory lift using equation (4).
4. Computation of Impulsive lift using equation (5).
5. Computation of Impulsive pitching moment using equations (6) and (7).
6. The total normal force and the effective total normal force are computed by equations (8) and (9) respectively.
7. The effective incidence is computed by using equation (10).
8. The unsteady separation vortex effects on the lift, position of center of pressure, and the pitching moment are computed by equations (12), (13) and (14).
9. Procedures (2-7) are repeated for a new time step.
10. Computations are terminated when the last time step is reached.

6. IMPLEMENTATION & DISCUSSION

The aerodynamic computational solution of the Navier Stokes equations was done using finite element method with help of ANSYS-5.8 to predict the static lift coefficient, pitching moment coefficient and the separation point for different angles of attack and surface roughness of NACA 0012 airfoil as shown in figures (6 to 8). To maintain the airfoil symmetric, the roughness of the upper and lower surface make with the same degree and position. The airfoil geometry with hypothetical surface roughness was drawn and translates the coordinate of each point into the ANSYS-5.8 computer software and applies the flow boundary conditions on the airfoil geometry.

Figure (6) shows the static lift coefficient curves of airfoil NACA 0012 at different surface roughness, the maximum lift coefficient will decreased with the airfoil surface roughness increase and also the stall angle decreased due to pressure loss, in which the stalling angle at ($R\approx0$) is 18.2º while at ($R=150\mu m$) is 16.2º. The static lift curve slope ($C_{L\alpha}$) is decreased slightly with the surface roughness increased. Figure (7) shows the static pitching moment coefficient curves of airfoil NACA 0012 at different surface roughness. The angle of attack corresponding to break in the static pitching moment is decreased with surface roughness. At ($R\approx0$) the break in the pitching moment occurs at about ($\alpha=16^o$) while at ($R=150\mu m$) it occurs at about ($\alpha=14^o$). Figure (8) illustrates the separation point curves of NACA 0012 airfoil for different surface roughness. As shown the separation will be moved toward the leading edge as the surface roughness increased. At 17º angle of attack for example the separation takes place at (0.348C) for smooth airfoil ($R\approx0$) while at ($R=150\mu m$) the separation takes place at (0.281C).

The influence of the surface roughness on the dynamic stall will be discussed in three cases as shown in figures (9, 10 and 11).

CASE-1: NACA 0012 AIRFOIL (α=12+8.5sinωt, K=0.1)

The calculated lift and pitching moment hysteresis loops at (M=0.3 and Re=2.4×10^6) of airfoil NACA 0012 with different surface roughness are presented in figure (9). In figure (9a), the upstroke region shows a similar behaviour with different surface roughness. The attached flow range between point (1-2), point 2 refers to the static stall angle. Above the static stall angle, the reversed flow developed, but the lift continuous to increase. At point 3 the reverse flow reaches the leading edge. At this point the moment stall begins as shown in figure (9b), but the lift is still increasing as a result of the separation vortex. At point 4 the maximum lift and moment occurred.

The maximum lift coefficient is 1.92 at 20º angle of attack for (R≈0), but it reachs to 1.67 with (R=150µm) surface roughness. This reduction in lift coefficient with increasing surface roughness is due to the dynamic stall vortex. The fully separated flow at point 5 occurs at about 19º for (R≈0) and at 17.5º for (R=150µm) surface roughness. Within the rang (5-6) the angle of attack decreases, with large hysteresis a boundary layer reattachment and a return to fully attached flow. For (R≈0º) the boundary layer reattachment occur at about 11º while at (R=150µm) surface roughness the boundary layer reattachment take place at about 9º as shown in figure (9a). The behaviour of the pitching moment coefficient for different surface roughness is presented in figure (9b). The moment stalls at point 3 about (-0.03) at 17º angle of attack for all, also for point 4 there is a reduction in maximum moment coefficient with increasing surface roughness.

CASE-2: NACA 0012 AIRFOIL (α=10+10sinωt, K=0.1)

Figure (10) represents the results at M=0.3 and Re=4×10^6. The general trend of the lift and moment hysteresis loops is predicted. Point 2 refers to the static stall angle at 14º with (R≈0) and at 13.3º for (R=150µm) surface roughness. At point 3 the lift stall takes place at 17.2 º incidences, point 4 refers to the stall at about 18.6º for (R≈0) and at 17.3º for (R=150µm). This is due to the pressure loss. Figure (10b) represents the behaviour of the pitching moment for this case. At point 4 there is a reduction in maximum pitching moment coefficient value with increasing surface roughness in which the absolute maximum difference is 0.15.

CASE-3: NACA 0012 AIRFOIL (α=15+10sinωt, K=0.15)

Figure (11) illustrate the calculated results at (M=0.3 and Re=3.5×10^6) of the lift and pitching moment coefficients loop. Figure (11a) represents the relationship between the lift coefficient and angle of attack for different surface roughness. The maximum lift coefficient is (2.4) at about (22.5º) angle of attack for (R≈0) and reaches to (1.7) at (R=150µm). This reduction in lift coefficient is due to the dynamic stall vortex. The behaviour of the relations is smooth during down stroke.

Figure (11b) represents the behaviour of the pitching moment coefficient with the angle of attack at different surface roughness. The pitching moment stall angle is about (20º) angle of attack for (R≈0) while the stall angle reach to (18º) at (R=150µm) surface roughness.

As the losses of some material from the airfoil surface leads to the surface roughness increased and then a reduction in the airfoil aerodynamic characteristics

take place, therefore a periodic test must be done on the airfoil surface and re-coating the surface if needed to avoid the reduction in the aerodynamic characteristics.

7. CONCLUSIONS

The effect of the airfoil surface roughness on dynamic stall of a rotary wing sections (NACA 0012) was studied using indicial method in which the static aerodynamic characteristics predicted numerically with help of ANSYS-5.8 software. The following conclusions are drawn:

1. The dynamic boundary layer reattachment takes place at smaller angle of attack than that smoother airfoil.
2. The maximum dynamic lift coefficient decreased when the airfoil surface roughness increases.
3. The dynamic stall angle decreases with an increase in airfoil surface roughness.
4. The maximum dynamic pitching moment coefficient decreases with an increase in airfoil surface roughness.

8. REFERENCES

[1] Ericsson L. E. and Reding J. P., "Dynamic Analysis in light of recent numerical and experimental results", Journal of aircraft, Vol. 13, No. 4, April 1976, pp. 248-255.

[2] Corten G. P., "Flow separation on wind turbine blades", ISBN 90-393-2582-0, NUGI 837, Netherland, January 2001.

[3] Geissler W. and Trenker M. T., "Numerical investigation of dynamic stall control by a Nose-Drooping device", American helicopter society, San Francisco CA, January-2002, pp. 23-25.

[4] Yousif A. H., Intesar A. A. and Abid A. B.," Effect of roughness on the performance of axial compressor cascade", AL-Rasheed Collage for Engineering and Science X/MEC, No. 4, 1989,pp. 75-89.

[5] McCroskey W. J. and Philippe J. J., "Unsteady viscous flow on oscillating", AIAA journal, Vol. 13, No. 1, January 1975, pp. 71-79.

[6] McCroskey W. J., "Some current research in unsteady fluid dynamics", ASME Journal of fluids engineering, Vol. 99, March 1977, pp. 8-38.

[7] McCroskey W. J. and Pacci S. L., "Viscous- inviscid interaction on oscillating airfoils in subsonic flow", AIAA Journal, Vol. 20, No. 2, February 1982, pp. 167-174.

[8] Vladislav K., Patrick C. M., Timothy J. C., and Jay M. B., "Analysis of Wind Tunnel Longitudinal Static and Oscillatory Data of the F-16XL Aircraft", NASA/TM-97-206276, December 1997.

[9] Shida Y., Kuwahara K. and Takami H., "Computation of dynamic stall of a NACA-0012 airfoil", AIAA Journal, Vol. 25, No. 3, March 1987, pp. 314-408.

[10] Abu-Tabikh, M. I., "Modeling of steady and unsteady turbulent boundary separation using vortex hybrid method", PhD thesis, University of technology, Baghdad, March 1997.

[11] Rae′d A. J., "Numerical study of dynamic stall controlled by Nose-Drooping technique", MSc. thesis, University of technology, Baghdad, February 2005.

[12] Beddoes T. S., "Representation of airfoil behaviour", AGARD specialists meeting on prediction of aerodynamic loads on Rotorcraft, AGARD CP-334, 1982.

[13] Leishman J. G. and Beddoes T. S., "A generalized model for airfoil, Unsteady aerodynamic behaviour and dynamic stall using the indicial method", Proceedings of 2nd annual forum of the American Helicopter society, Washington D. C., June 1986.
[14] Leishman J. G. and Nguyen K. Q., "Static-space representation of unsteady airfoil behaviour", AIAA Journal, Vol. 28, No. 5, March 1990, pp. 836-844.
[15] Ballhaus W. F and Goorjian P. M., "Computation of unsteady transonic flows by the indicial method", AIAA Journal, Vol. 16, No. 2, March 1978, pp. 117-124.
[16] Dowell E. H., Curtiss Jr. H., Scanlan R. H. and Sisto F., "A modern course in aeroelasticity", Sijthoff and Noordhoff, 1980.
[17] Sears W. R., "Operational methods in the theory of airfoils in non-uniform motion", Journal of the Franklin Institute, Vol. 230, No. 1, July 1940, pp. 95-111.
[18] Leishman J. G., "Indicial lift approximation for two-dimensional subsonic flow as obtained from oscillatory measurements", Journal of aircraft, Vol. 30, No. 3, May 1993, pp. 340-351.
[19] Beddoes T. S., "A synthesis of unsteady aerodynamic effects including stall hysteresis", Proceeding of 1st European Rotorcraft forum, Southampton, September 1975.
[20] Robert L. Norton, "Machine Design An Integrated Approach" Prentice-Hall, London, 1998.

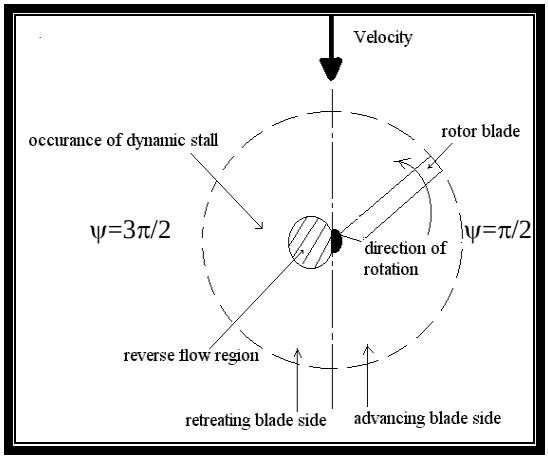

Figure (1): Helicopter rotor disc [2].

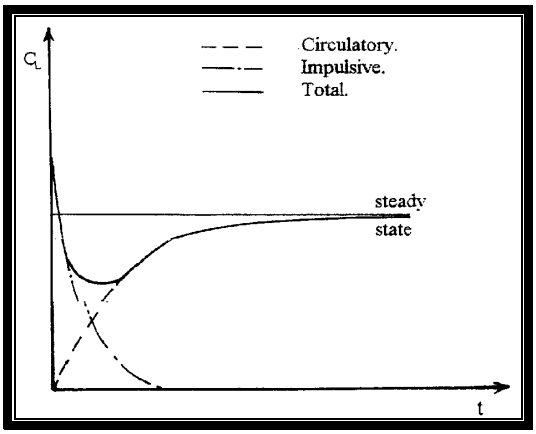

Figure (2): Total indicial lift response to a step change in angle of attack [13].

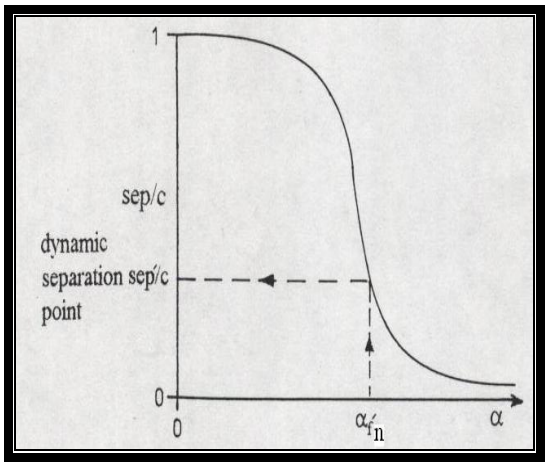

Figure (3): Variation of separation point with angle of attack for the static case [13].

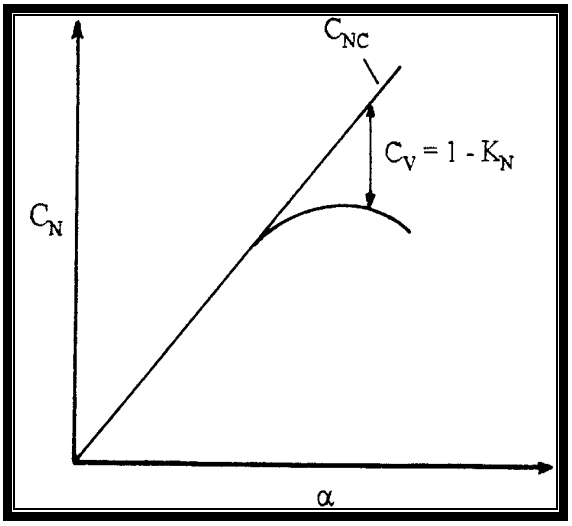

Figure (4): Modeling of vortex lift [13].

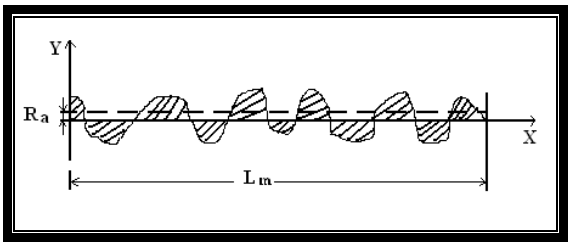

Figure (5): Arithmetic mean roughness value [20].

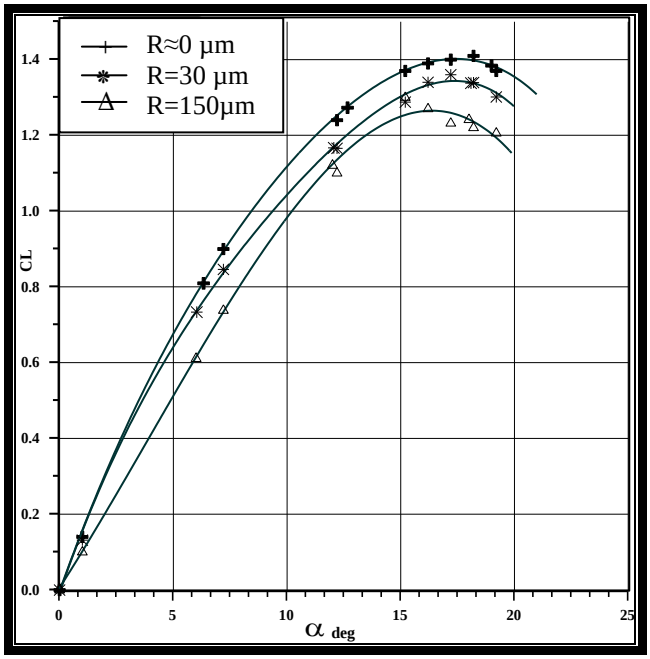

Figure (6): Static lift curve of airfoil NACA 0012 at different surface roughness.

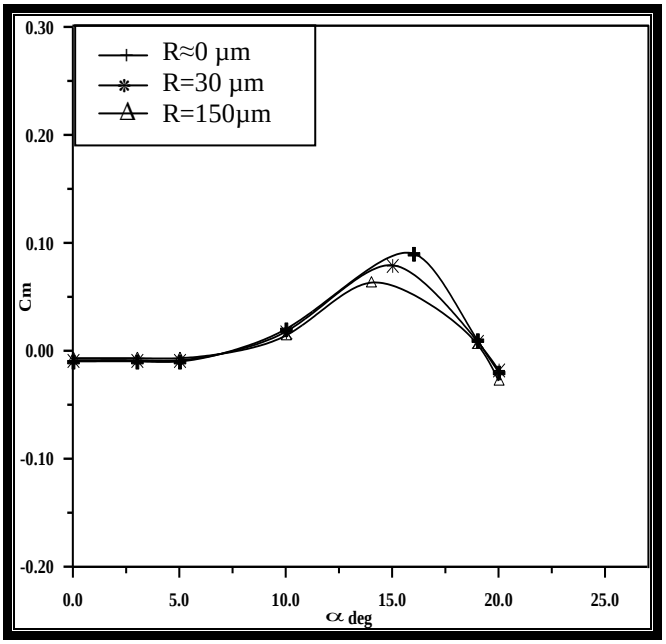

Figure (7): Static pitching moment curve of airfoil NACA 0012 at different surface roughness.

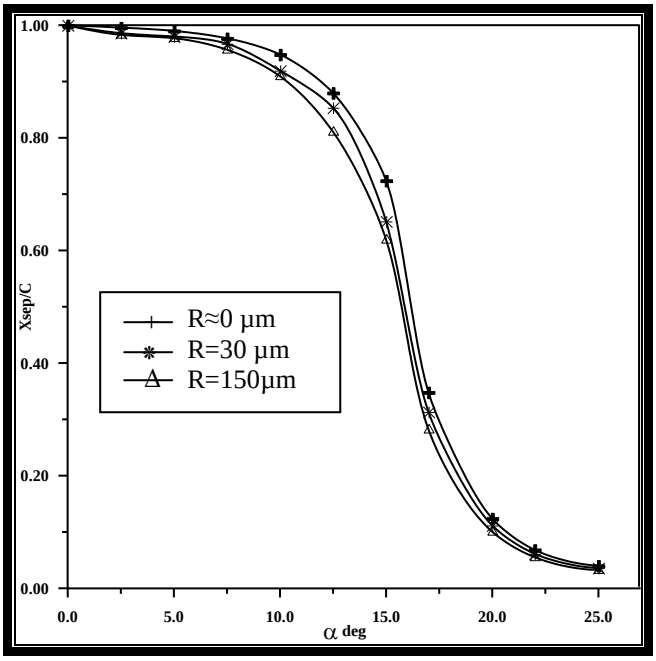

Figure (8): Separation point curve of airfoil NACA 0012 at different surface roughness.

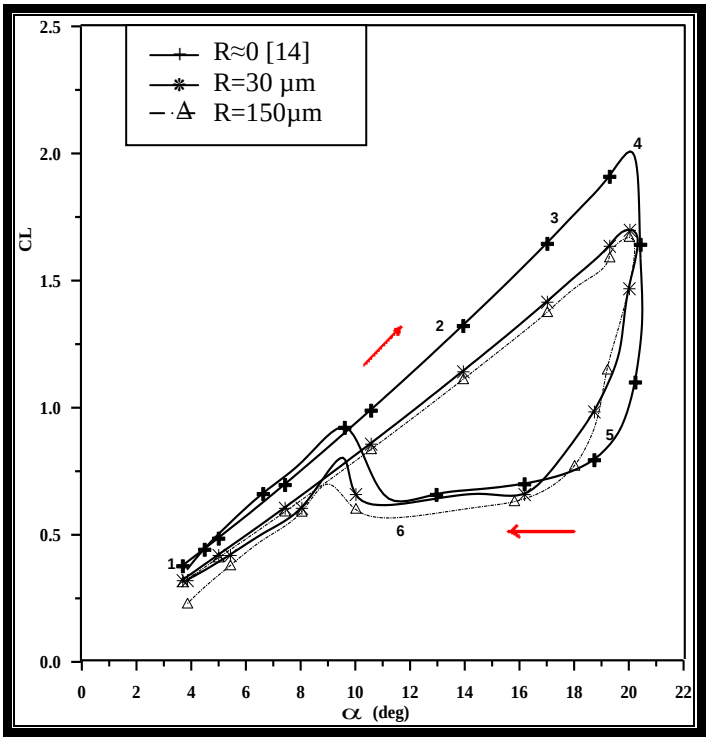

a. Lift hysteresis loop

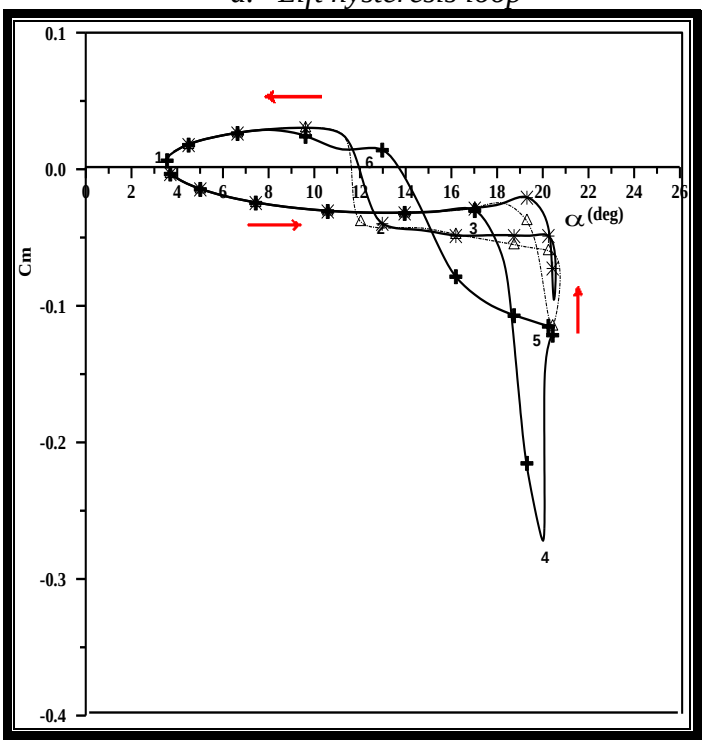

b. Pitching moment hysteresis loop

1 -Boundary layer flow reverses.
2 -Formation of separation vortex.
3 -Maximum normal force.
4 -Maximum negative moment.
5 -Fully separated flow.
6 –Boundary layer reattaches front to rear.

Figure (9): Effect of surface roughness on Unsteady lift and pitching moment coefficients for the NACA 0012 airfoil in the dynamic stall regime (α=12+8.5sinωt, K=0.1, x_o/c=0.25).

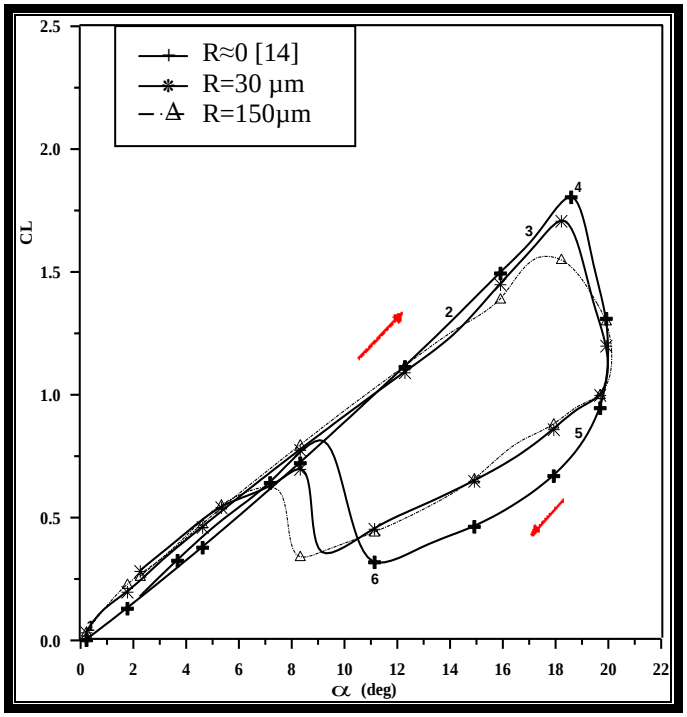

a. Lift hysteresis loop

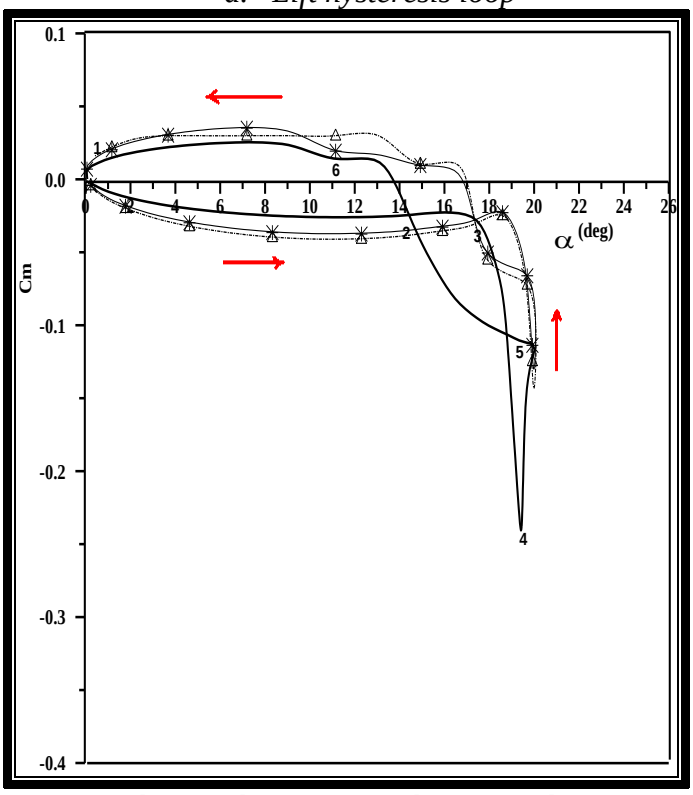

b. Pitching moment hysteresis loop

Figure (10): Effect of surface roughness on Unsteady lift and pitching moment coefficients for the NACA 0012 airfoil in the dynamic stall regime (α=10+10sinωt, K=0.1, x_o/c=0.25).

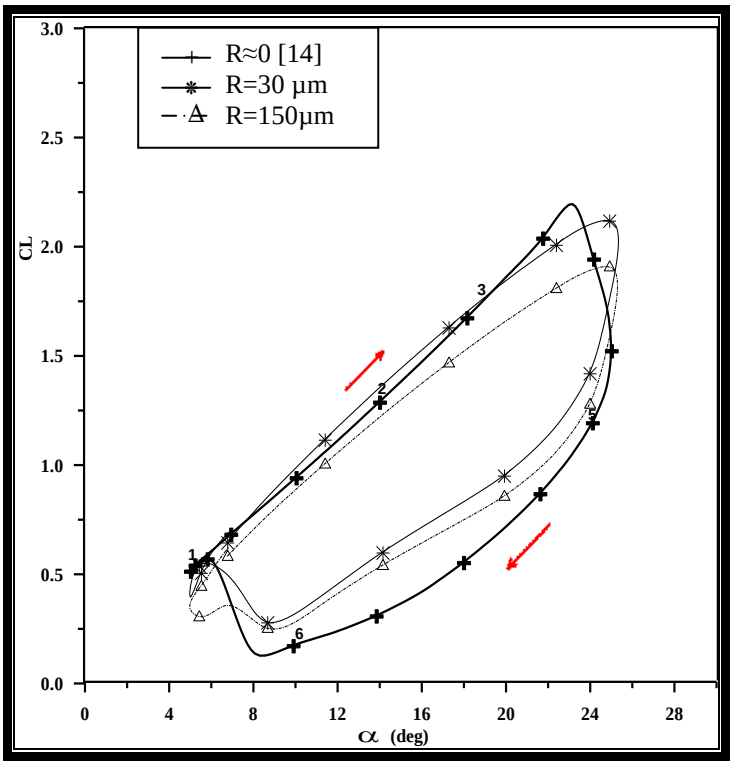

a. Lift hysteresis loop

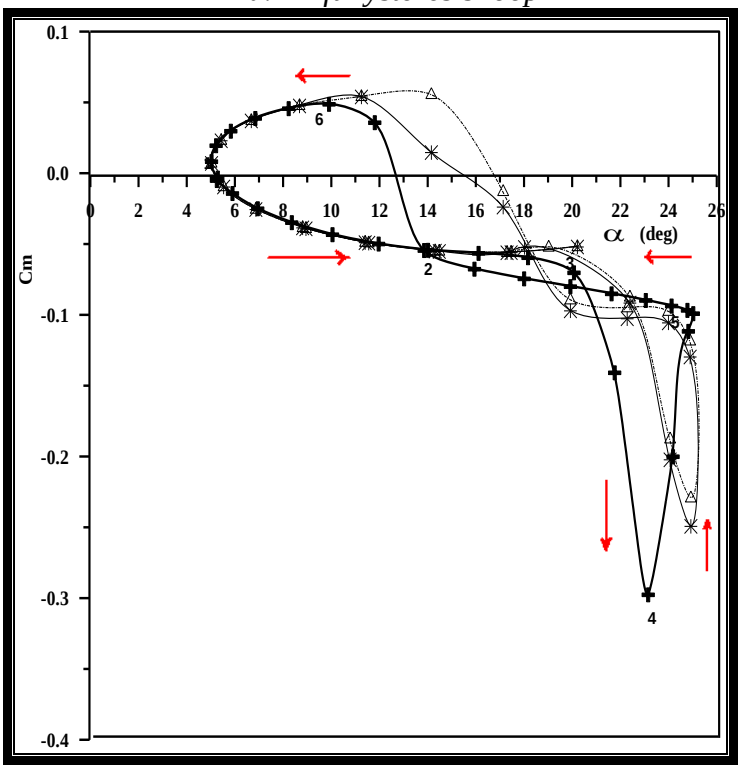

b. Pitching moment hysteresis loop

Figure (11): Effect of surface roughness on Unsteady lift and pitching moment coefficients for the NACA 0012 airfoil in the dynamic stall regime (α=15+10sinωt, K=0.15, x_o/c=0.25).

تأثير خشونة السطح على ظاهرة الأنهيار الديناميكي لمقطع جناح دوار عند الجريان تحت الصوتي

الدكتور المهندس فرج محل محمد*

المستخلص

في هذا البحث تمت دراسة تأثير خشونة السطح على ظاهرة الأنهيار الديناميكي لمقطع جناح دوار عند الجريان تحت الصوتي. استخدم معدل القيمة الحسابية لمعرفة خشونة سطح المقطع وفق النظام العالمي (ISO-4287/1) . تم استخدام طريقة الاستجابة القرائنية للجريان غير المستقر ثنائي الأبعاد لحساب الرفع والعزم غير المستقر لمقطع جناح نوع (NACA 0012) تحت تذبذب العزم في نظام انهيار ديناميكي عالي. استخدم برنامج ANSYS-5.8على الحاسبة للحصول على المعطيات الستاتيكية المطلوبة في الطريقة القرائنية. تمت دراسة العديد من الحالات المختلفة وتضمنت النتائج التصرف المعتمد على الزمن على شكل حلقات للرفع والعزم المتكون من استخدام خشونة مختلفة لمقطع الجناح. وبينت نتائج الاسطح الخشنة ان معامل الرفع يقل ونقطة الانفصال تتقدم الى الامام باتجاه الحافة الامامية وان اعادة طبقة الانفصال تحصل عند زوايا صغيرة وان زاوية الانهواء تقل وعزم التأرجح يقل بالمقارنة مع الاسطح الاكثر نعومة وعليه يجب اجراء الفحص الدوري للريش الدوارة لمعرفة خشونة السطح واعادة طلائها كلما استوجب ذلك.

*الجامعة التكنولوجية/ قسم التعليم التكنولوجي.